Sustainable Chemical Engineering
http://ojs.wiserpub.com/index.php/SCE/

UNIVERSAL WISER PUBLISHER

Research Article

Design of Experiments for Increasing of Methylene Blue Adsorption onto Cellulose Derivative-Based Composites

M. A. Silva

Center for Science and Technology, Department of Textile Engineering, University of Minho, 4800-058, Guimarães, Portugal
Email: mabsilva2013@gmail.com

Received: 28 December 2023; **Revised:** 29 January 2024; **Accepted:** 21 February 2024

Abstract: Hematite-cellulose acetate composite membranes (M1, M2, and M3) were evaluated for their performance in Methylene Blue (MB) adsorption. The Box-Behnken design was used to evaluate the influence of operational parameters on the adsorption of MB by these adsorbents. The idea was to optimize the process with maximum efficiency in adsorption, through identification of the influential factors in the process, evaluation of interactions between these factors, and modeling mathematical expressions. Adsorption experiments versus time were better described by the non-linear pseudo-first-order model, followed by the pseudo-second-order model, and then the linear pseudo-first-order model. The R^2 and chi-square values corroborate this finding. Equilibrium data were also evaluated and modeled using the linear and non-linear Langmuir and Freundlich isotherm models. The linear isotherm models were more suitable to fit the adsorption equilibrium data on the membranes, followed by the non-linear Langmuir model. Thus, it was presumed that chemisorption was the prevailing adsorption mechanism. Additionally, adsorption proved to be exothermic and spontaneous. A quadratic model equation was found to describe the interaction between factors. The coefficients of pH and MB concentration were positive, thus positively affecting the adsorption of MB, but those of temperature were negative, justifying the negative effect on the adsorption process. Analysis of Variance (ANOVA) showed a high coefficient of determination value, and a high predictive power of the regression model was derived. The highest adsorption capacity was found at the optimum experimental conditions of pH = 9.0, MB initial concentration = 100 $mg \cdot L^{-1}$, and temperature = 20 °C. Finally, the composites provided five use cycles, which is good when considering the adsorbents used in removing textile dyes from wastewater.

***Keywords*:** cationic dye removal, methylene blue, hematite-cellulose acetate membrane, adsorption kinetics, equilibrium isotherms, Box-Behnken design

1. Introduction

Dyes are molecules used in considerable amounts by textile, pharmaceutical and paint industries, due to their strong colouration in solution and fixation to materials. However, these industrially related synthetic dyes are hazardous, toxic and difficult to remove from water, and thus considered as emerging contaminants. With the world population increasing and natural resources becoming scarce, it is urgent to have ecological processes (dyeing and painting) and updated reports of leached dyes. It is known that even at low concentrations they are harmful to humans and aquatic organisms and, therefore, huge efforts have been done to increase the effectiveness of remediation procedures and development of

DOI: https://doi.org/10.37256/sce.5120244174

new methods for their detection and quantification according to the required quality of water for human consumption, livestock and irrigation.[1-3] Even though the numerous efforts made in the last 20 years, the problem continues to be a major concern for academics and governments as numerous catastrophes have been occurring around the globe. Various guidelines have been published,[4-6] but the complexness of water which contains a wide variety of molecules, ions and dissolved microorganisms makes purification and its reuse very challenging, particularly in developing countries. Even so, it is our responsibility to continue making efforts to reduce pollution and, whenever possible, prevent it from leaching.

Methylene blue (MB) is a cationic synthetic dye commonly applied for dyeing fabrics, papers and leathers.[7] Additionally, it is used in the food and pharmaceutical industries.[8] Although MB has a large spectrum of applications, it can possess several risks due to the release of partially untreated MB-loaded wastewater from the aforementioned industries. For example, in humans, MB dye can induce various ailments such as cyanosis, tissue necrosis, Heinz body formation, vomiting, jaundice, shock, and enhanced heartbeat rate, amongst others.[9] Also, with respect to plants, the presence of MB has become a major challenge, such as growth inhibition, reduction of pigment, etc.[10] Thus, the negative effects of MB-loaded wastewater have been one of the major environmental concerns of academics and policy makers who demand urgent removal prior to industrial discharge.

Assorted treatment methods, including biological methods, chemical methods, and physicochemical methods have been widely applied to eliminate dyes from the environment.[11] However, most of them are energy-demanding and time-consuming compared to the adsorption process.[12-15] The adsorption process based on membranes and fibers is effective in dye separation, but the related investment could be relatively high due to membrane fouling. Still, adsorption is a better option in terms of energy consumption, simplicity of design and operation, availability of adsorbents, effectiveness and the lack of sensitivity to toxic substances compared to other methods.

In our previous work, we focused on the adsorption process made by cellulose acetate composites, since cellulose acetate (CA) is an environment-friendly and biodegradable regenerated cellulose material, which can be bought in many sellers as powder and can be fabricated as semipermeable membranes. Firstly, we used carbon nanoparticles[12,16] and then we adopted the iron oxide nanoparticles.[17-18] Both nanoparticles showed good physicochemical properties such as optical, semiconducting, ferromagnetic and antimicrobial activity against common strains. However, the iron oxide nanoparticles proved to be more effective for the functionalization of cellulose acetate due to its lower cost of production, simplicity of manipulation and greater physicochemical properties. Therefore, this work focused on the use of previously synthesized hematite-cellulose acetate composites as adsorbents, in the form of films formed by phase inversion methodology, for the removal of MB from a model wastewater. From our previous work,[12,18] we know the dual advantages of these membranes: adsorbents and filters. Here, the cellulose-based materials are being used as adsorbents and, subsequently, will be tested as filters (permeability, fouling and selectivity will be analysed). Even though MB is a model dye and numerous papers refer to it, we know that little information is available on the removal of MB by adsorption onto hematite-cellulosic materials.

This paper is divided into two parts. The first part involves the adsorption kinetics and equilibrium isotherms studies, and the second regards to design of experiments (DoE) to show the combined effects of experimental factors (pH, initial MB concentration, and temperature) on the capacity of adsorbents. Design of experiments (DoE) is a technique that involves appropriate experimental designs, mathematical equations and graphical results.[19-20] Box-Behnken Design (BBD) is one type of DoE widely used for optimization as it allows for the consideration of factors at three levels and ensures that all design points are within the safe operating zone. It is also more proficient and powerful than other designs[21-23] as it requires fewer experimental runs than the three-level full factorial design and the central composite design (CCD).

The objective of this work is to show the high performance of cellulose-based composite membranes as adsorbents and alternatives to another adsorbent, revealing their potential application in wastewater treatment, and develop mathematical models based on the effects of the operational parameters (pH, dye concentration, temperature) on the adsorption of MB on a cellulosic composite, and then to optimize the response using response surface designs.

2. Experimental

2.1 *Reagents and equipments*

All chemicals were of analytical grade from Merck (Darmstadt, Germany) and used as received.

Pristine/cellulose acetate membrane (M0) and composite/hematite-cellulose acetate membranes (M1, M2 and M3) were synthesized and fully characterized as described by us, previously.[17] Methylene blue dye was dissolved in ultra-pure water to create a stock solution of MB at the concentration of 1,000 mg × L^{-1}. The working solutions were diluted using the stock solution. The pH of the aqueous MB solution was controlled using 0.1 M HCl and 0.1 M NaOH solutions. pH measurements were done with a digital pH meter (pH meter/ISE Thermo Orion Dual Star, Thermo Scientific Orion, Alvarado, TX, USA). After pH adjustment, the concentration of MB in the solution was measured using a UV-Vis spectrophotometer (UV-2600, Shimadzu Europa GmbH, Duisburg, Germany).

2.2 *Dye removal experimental analysis*

A first set of experiments was conducted in batch mode to investigate the effects of MB initial concentration, pH and temperature on the removal efficiency of the adsorbents. pH effect was evaluated in the pH range of 3 to 9, with other parameters constant (initial MB concentration = 100 mg × L^{-1}; adsorbent dose = 25 mg; contact time = 300 min and temperature = 25 °C). MB initial concentration effect was studied in the concentration range of 40 to 100 mg × L^{-1} (pH = 7; adsorbent dose = 25 mg; contact time = 300 min and temperature = 25 °C). Temperature effect on adsorption was studied in the range of 20 to 30 °C (initial MB concentration = 100 mg × L^{-1}; pH = 7; adsorbent dose = 25 mg; contact time = 300 min). All experiments were performed in triplicate.

Additional experiments were done to study the adsorption kinetics. They were conducted in 25 mL of an MB solution with a concentration of 100 mg × L^{-1} and a pH of ~ 7. An amount of 25 mg of adsorbents was mixed with the dye solution in a series of plastic bottles. The bottles were shaken at 120 rpm for 300 min, in a thermostatic bath, until equilibrium. At different time intervals, samples were collected, and filtered using a 45 µm filter paper and the concentration of MB in the working solution was measured pH was measured.

2.3 *Dye concentration in function of time*

The dye concentration in the working solution was determined through spectrophotometric analysis at a wavelength (λ_{max}) of 668 nm. Equation 1 was used to calculate the adsorption capacity (mg × g^{-1}) of the adsorbents, where C is the dye concentration at equilibrium time (300 min), m is the weight of the adsorbent (25 mg) and V is the adjusted volume in dye solution (initial volume of 25 mL). The percent dye removal (R, %) was calculated using Equation 2, where C_0 is the initial concentration of MB (mg × L^{-1}) and C_e is the concentration of MB at equilibrium (mg × L^{-1}) in the bottles.

$$q = \frac{C \times m}{V_{adj}} \tag{1}$$

$$R(\%) = \frac{C_0 - C_e}{C_0} \times 100 \tag{2}$$

2.4 *Design of experiments by box-behnken design (DoE-BBD)*

To analyze and optimize the operating conditions on the removal efficiency of MB, a factorial design was used. Response surface methodology (RSM) was adopted as it allows to estimation of interaction between factors and quadratic effects, giving an idea of the contour of the response surface. For an RSM problem involving three factors (X_1: pH, X_2: initial dye concentration and X_3: temperature) and three levels (high, middle and low), the Box-Behnken design (BBD) is the most efficient. 15 experimental runs with three central points were performed to find out the experimental error and precision of the design. Minitab software version 17.1.0 (file name: mtben1710ac.exe) was used to run the 15 experimental runs. The response was the adsorption capacity of MB onto membranes (q, mg × g^{-1}) after equilibrium time. Table 1 shows the three-level parameters and Table 2 shows the details of the experimental runs for each adsorbent

(M0, M1, M2 and M3). The results obtained for the response were fitted to a quadratic polynomial model explained by the non-linear Equation 3, where Y was the measured response, A_0-A_9 were regression coefficients, and X_1, X_2, and X_3 were the studied factors (independent variables). To validate the fitted model, Analysis of Variance (ANOVA) was applied. The precision of the fitted polynomial model was confirmed by the high correlation coefficient (R^2) value, and a 95% confidence interval was used to evaluate the p-value ($Prob > F$) and check the significance of the model.

$$Y = A_0 + A_1X_1 + A_2X_2 + A_3X_3 + A_4X_1X_2 + A_5X_2X_3 + A_6X_1X_3 + A_7X_1^2 + A_8X_2^2 + A_9X_3^2 \quad (3)$$

Table 1. Process factors and their levels

Factors	Actual Levels		
	Low (-1)	Middle (0)	High (+ 1)
X_1: pH	3	6	9
X_2: Dye Concentration (mg × L^{-1})	40	60	100
X_3: Temperature (°C)	20	25	30
Response	Y: Adsorption capacity (mg × g^{-1})		

Table 2. Detail experimental runs for Box Behnken Design (BBD) with factor values in the coded form and respective responses/output

Run	Independent variables (X)			Dependent variable (Y)			
	X_1	X_2	X_3	M0	M1	M2	M3
1	-1	-1	0	5.2	1.1	1.2	0.7
2	1	-1	0	21.1	30.1	39.1	27.5
3	-1	1	0	18.1	0.1	0.2	0.1
4	1	1	0	44.3	55.5	71.4	50.4
5	-1	0	-1	15.5	1.2	1.4	1.1
6	1	0	-1	33.9	47.1	58.4	45.1
7	-1	0	1	7.9	0.5	0.6	0.3
8	1	0	1	24.2	35.3	46.7	29.8
9	0	-1	-1	19.5	18.8	22.8	17.4
10	0	1	-1	37.4	44.6	55.4	31.3
11	0	-1	1	12.2	11.2	18.7	10.1
12	0	1	1	28.5	23.5	35.7	22.8
13	0	0	0	21.8	27.3	49.4	25.1
14	0	0	0	21.8	27.3	49.4	25.1
15	0	0	0	21.8	27.3	49.4	25.1

3. Results and discussion

The main physicochemical properties of adsorbents (M0, M1, M2 and M3) are presented in Table 3 which were advertised in a previous publication.[17] In order to spread out the applicability of these adsorbents for different dyes, they were tested for MB, which is commonly used as a model dye in adsorption studies. The obtained results will help

us in the subsequent studies with cellulose composites as filter membranes in a pilot-scale process. To understand the adsorption mechanism, which depends on the specific adsorbent, adsorbate and reaction parameters,[24] the following analysis was performed.

Table 3. Physicochemical properties of the adsorbents[17]

Adsorbent/Membrane	pH (± SD)	Porosity (%, ± SD)	Textural properties
M0	1.8 ± 0.5	50 ± 2	The surface at the top was rougher, and there were valleys at the bottom surface. In addition, both microvoids and macrovoids were identified in the sublayer
M1	5 ± 0.5	75 ± 3	The surface at the top was rougher, and the sub-layer contained a structure primarily composed of macrovoids. Additionally, nanoparticles of hematite were found on the surface
M2	5.5 ± 0.4	72 ± 4	
M3	6 ± 0.4	80 ± 3	

3.1 *Factors affecting the adsorption capacity*

MB has a pKa value of about 5.6.[25] Above the pH value of 6, cationic MB molecules are the dominant species in solution. On the other hand, the point of zero charge (pH_{PZC}) for each membrane, which defines the pH value at which the surface charges of the adsorbent is zero, was lower than 7 as shown in Table 3. Thus, at a pH > 7 the surface charge of the adsorbents was negative, and the adsorption of MB onto the surface of the membranes was enhanced due to the opposite charges between the adsorbent and the adsorbate. A similar behaviour was discussed by us previously.[18]

Figure 1(a) represents the effect of pH on the adsorption capacity of each membrane. The maximum adsorption was achieved at pH = 9.0 with removal efficiencies of 44.5% for M0, 55% for M1, 71.4% for M2 and 50.4% for M3, after 300 minutes at 25 °C. A common situation was observed before[18] due to an increase in the electrostatic interactions between cationic dye molecules and negative surface charge on adsorbents. It is known that at pH < pH_{PZC}, the adsorbent surface was positively charged, and the interactions between MB and composite membranes were smaller due to the protonation of carboxyl groups belonging to the cellulose backbone. At a pH > pH_{PZC}, the carboxyl groups de-protonated and became negatively charged, increasing the interactions with the predominantly cationic MB species. The effect of pH on the adsorption capacity of charged adsorbents is well documented in the literature.[13,14,25-27]

Figure 1(b) shows the effect of contact time on the adsorption capacity for each membrane. The adsorption of MB (initial dye concentration: 100 mg × L^{-1}) was studied in the range of 0 to 300 minutes, using 25 mg of adsorbent at 25 °C and a pH = 7. At first, the adsorption rate increased rapidly and gradually slowed down until reaching equilibrium.[18] This is explained by the fact that adsorption in the first place occurred on the external surfaces of the composite, resulting in a fast adsorption rate, and with surface saturation MB gradually diffused into the interior of pores, which produced a decrease in the adsorption rate.[18,26,28]

As shown in Figure 1(b), the maximum removal efficiency was achieved within 240 to 300 minutes, without further change in the equilibrium adsorption capacity (q_e) after 300 minutes. 300 minutes was considered to be an effective equilibrium time for adsorption. The q_e values for M0, M1, M2, and M3 were found to be 40.9, 49.5, 69.0, and 41.5 mg MB × g^{-1} of loaded membrane, respectively. The lower q_e values observed for M1 and M3 are attributed to the porosity and surface chemistry of the adsorbents as reported on Table 3.

Figure 1(c) illustrates the effect of MB initial concentration on the adsorption behaviour. As the MB concentration increased, adsorption capacity on the surface of the adsorbent also increased because of the available groups on the adsorbents to form bonds (carboxyl and hydroxyl groups from composites structure). However, this trend was not systematic and the MB removal reached its highest value at a concentration of 100 mg × L^{-1}. After this value, the efficiency decreased possibly due to the excess of solute, which led to competition effects between MB molecules and the aggregation. Normally, this produces an exhaustion of the accessible activated sites on the adsorbent surface.[29]

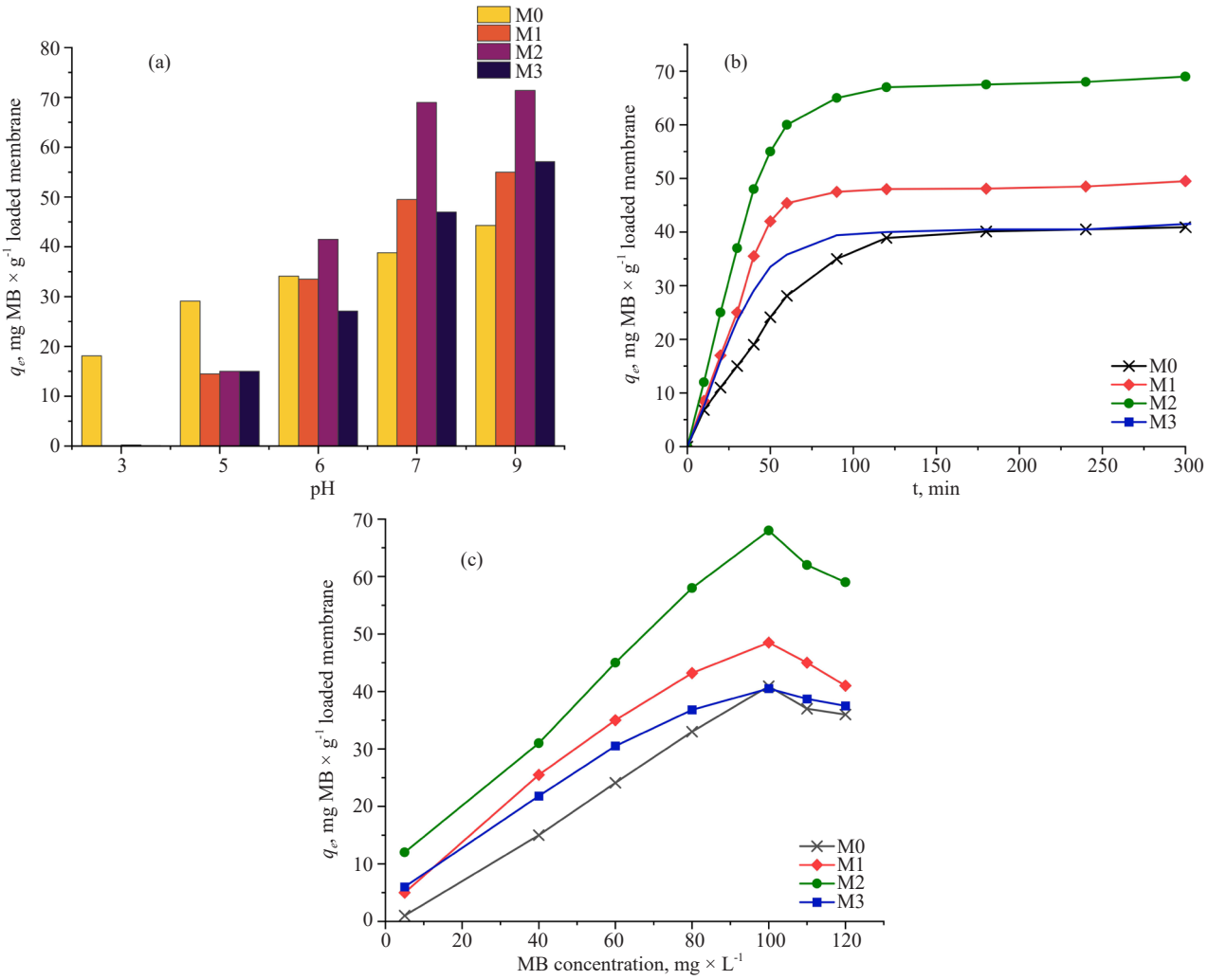

Figure 1. The effect of parameters on the adsorption of MB: (a) pH (initial dye concentration = 100 mg × L^{-1}; membranes = 25 mg; t = 300 min; T = 25 °C); (b) contact time (initial dye concentration = 100 mg × L^{-1}; membranes = 25 mg; pH = 7; T = 25 °C); and, (c) initial concentration of MB (contact time = 300 min; membranes = 25 mg; pH = 7; T = 25 °C)

3.2 *Linear and non-linear kinetic models*

3.2.1 *Linear and non-linear pseudo-first-order (PFO) and pseudo-second-order (PSO)*

After integration by using the boundary conditions $q_t = 0$ at t = 0 and $q_t = q_t$ at t = t, Equations (4) and (5), may be rearranged to obtain the linear and non-linear forms of kinetic equations (equations (6)-(9)), Table 4 linear regression was the frequently used method to determine the best-fitted kinetic model and its parameters. Equation (4) represents the pseudo-first-order (PFO) kinetic equation proposed by Lagergren,[30] and equation (5) defines pseudo-second-order (PSO) kinetic equation proposed by Blanchard,[31] developed by Ho,[32] and finally derived theoretically by Azizian.[33]

$$\frac{dq_t}{dt} = k_1\left(q_e - q_t\right) \tag{4}$$

$$\frac{dqt}{t} = k_2\left(q_e - q_t\right)^2 \tag{5}$$

The linear forms of the PFO and PSO equations were widely used to determine the most fitted kinetic model for the adsorption process. When using the linear form, experimental adsorption kinetics should be linearized for the

linear least-squares regression to estimate the model parameters. It has been shown that transformations of non-linear equations to linear forms implicitly alter their error structure in the measurement of model parameters.[34-35] All the equations in Table 4 used the software Origin 2024 (free trial license) to determine the linear and non-linear regression. It should be mentioned that the value of q_e used to fit Equations (6) and (7) was an experimental value ($q_{e,\,exp}$) taken from the equilibrium adsorption study. The non-linear forms of both models are presented in Equations (8) and (9).

$$\ln\left(q_e - q_t\right) = \ln q_e - k_1 t \tag{6}$$

$$\frac{t}{q_t} = \frac{1}{k_2 q_e^{\,2}} + \frac{t}{q_e} \tag{7}$$

$$q_t = q_e \times \left(1 - e^{-k_1 \times t}\right) \tag{8}$$

$$q_t = \frac{k_2 \times q_e^{\,2} \times t}{1 + k_2 \times q_e \times t} \tag{9}$$

Figures 2(a)-(d) show the comparisons of the adsorption kinetics of MB on each membrane for fitting the experimental data with the linear and non-linear model forms. The kinetic parameters, the correlation coefficient (R^2) and the adjusted chi-square (c^2) obtained from the linear and no-linear fittings are listed in Table 4.

Figures and values show that the PSO model was better than the PFO model in the fitting of the kinetics of MB adsorption on membranes. The values of R^2 were greater than 0.98, Chi-square was between 0.055 and 0.070, and a good agreement between the experimental adsorption capacity ($q_{e,\,exp}$) and the calculated adsorption capacity ($q_{e,\,cal}$) values. The adsorption capacity calculated by the PSO model was 50.50 mg MB × g^{-1} on M0, 55.87 mg MB × g^{-1} on M1, 78.12 mg MB × g^{-1} on M2 and 46.30 mg MB × g^{-1} on M3, which are approximate to the experimental data. The PSO model has been extensively used to describe chemisorption involving valency forces through the sharing or exchange of electrons between the adsorbent and adsorbate as covalent forces and ion exchange.[36]

Even though the linear results suggested the PFO model be discarded, the non-linear form of the model fitted in good agreement with the experimental data, as indicated by better R^2 and approximate q_e values (Figure 2 (c) and (d); Table 4). In spite of erratic adsorption rate behavior, the calculated adsorption at equilibrium was found a little lower (42.03 mg MB × g^{-1} on M0, 50.10 mg MB × g^{-1} on M1, 69.58 mg MB × g^{-1} on M2 and 41.50 mg MB × g^{-1} on M3) but much approximated to experimental data than that recorded with the linear model. Even though, the Chi-square values were a little higher than the Chi-square values obtained for the linear fit. Consequently, the PFO non-linear model properly predicted the equilibrium adsorption capacity for the adsorption kinetics of hematite-cellulose membranes. On the contrary, the PSO non-linear model was demonstrated to be not so good at describing the kinetics.

3.2.2 *Elovich model*

The Elovich equations (Equations (10) to (12)) are given below. The exponential Elovich (origin Elovich model) equation[37] has general application to chemisorption kinetics and has been used to describe the kinetics of heterogeneous exchange reactions.[38]

$$\frac{dqt}{t} = A\exp\left(-Bq_t\right) \tag{10}$$

$$q_t = \frac{1}{B} \times \ln\left(AB\right) + \frac{1}{B} \times \ln\left(t\right) \tag{11}$$

$$q_t = \frac{1}{B} \times \ln\left(1 + ABt\right) \tag{12}$$

Herein, the Elovich model did not fit kinetic adsorption onto composite membranes (Figures 2 (e) and (f), Table 4). Kinetic parameters and statistical values of R^2 and Chi-square were extremely inappropriate which confirms the

unsuitability of Elovich models (linear and non-linear) for the experimental data.

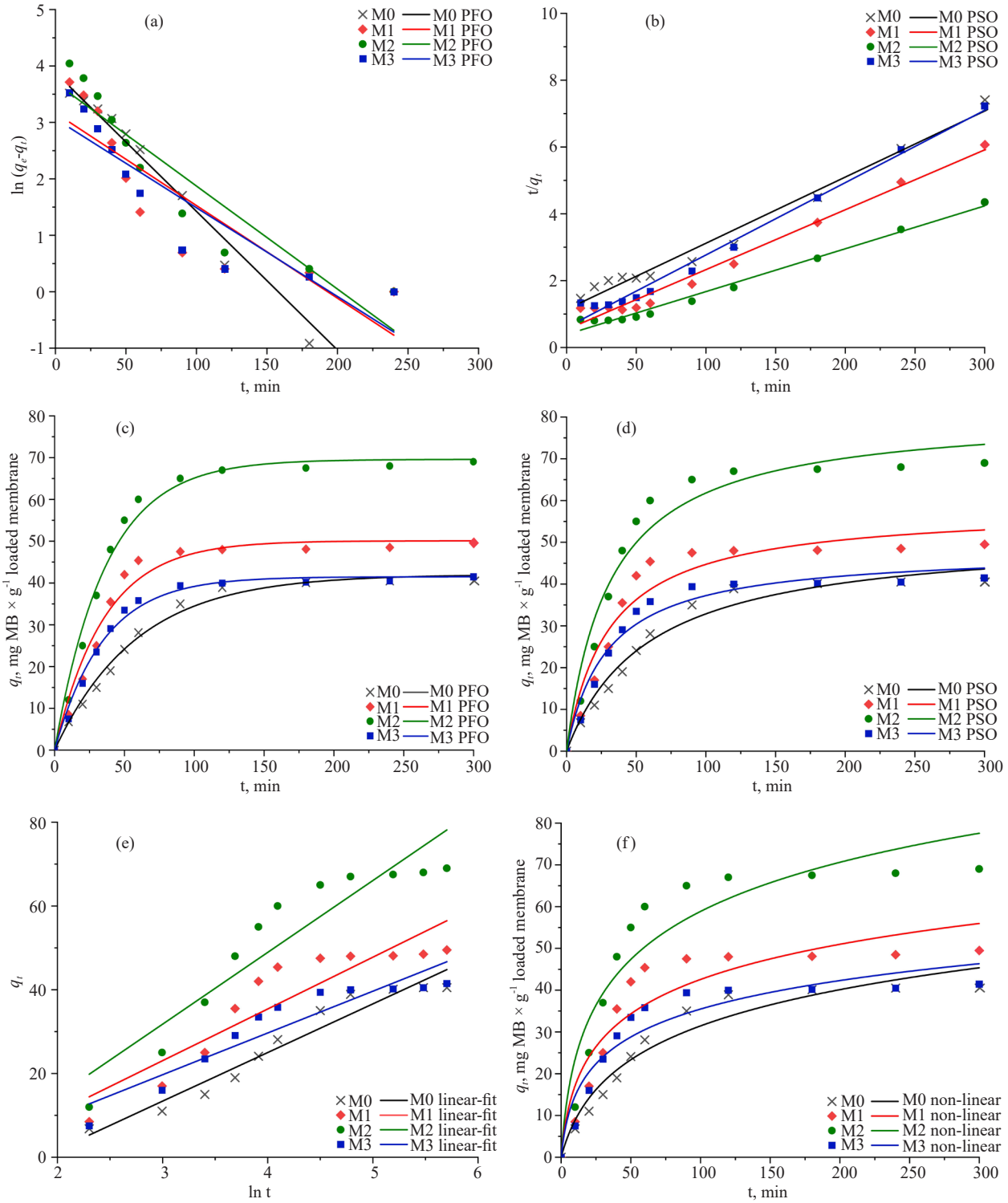

Figure 2. Experimental data and the fitted linear and non-linear kinetic models: (a) linear PFO; (b) linear PSO; (c) non-linear PFO; (d) non-linear PSO; (e) linear Elovich; and (f) non-linear Elovich (initial dye concentration = 100 mg × L^{-1}; pH = 7.0; membranes = 25 mg; contact time = 300 min; T = 25 °C)

Table 4. Parameters calculated from linear and non-linear kinetic models (initial MB concentration = 100 mg × L^{-1}, membranes = 25 mg, pH = 7.0, temperature = 25 °C)

Linear PFO	k_1, min^{-1}	R^2	$q_{e,exp}$ mg × g^{-1}	$q_{e,cal}$ mg × g^{-1}	χ^2
M0	0.0246	0.98	40.50	48.49	0.0606
M1	0.0164	0.77	49.51	23.74	0.4145
M2	0.0183	0.88	69.02	40.50	0.2350
M3	0.0157	0.82	41.53	21.35	0.2825
Linear PSO	k_2, g × mg^{-1} min^{-1}	R^2	$q_{e,exp}$ mg × g^{-1}	$q_{e,cal}$ mg × g^{-1}	χ^2
M0	3.43E-4	0.98	40.50	50.50	0.0704
M1	5.98E-4	0.98	49.51	55.87	0.0600
M2	4.21E-4	0.98	69.02	78.12	0.0231
M3	7.74E-4	0.99	41.53	46.30	0.0553
Non-linear PFO	k_1, min^{-1}	R^2	$q_{e,exp}$ mg × g^{-1}	$q_{e,cal}$ mg × g^{-1}	χ^2
M0	0.0172	0.99	40.50	42.03	2.095
M1	0.0282	0.97	49.51	50.10	9.636
M2	0.0274	0.99	69.02	69.58	7.893
M3	0.0288	0.99	41.53	41.50	2.307
Non-linear PSO	k_2, g × mg^{-1} min^{-1}	R^2	$q_{e,exp}$ mg × g^{-1}	$q_{e,cal}$ mg × g^{-1}	χ^2
M0	3.26E-4	0.97	40.50	52.16	5.939
M1	5.63E-4	0.94	49.51	58.33	21.51
M2	3.95E-4	0.96	69.02	81.08	25.35
M3	7.14E-4	0.96	41.53	48.06	8.327
Linear Elovich	A, mg × g^{-1} min^{-1}	B, mg × min^{-1}	R^2		χ^2
M0	1.832	0.0861	0.94		8.976
M1	3.974	0.0809	0.83		35.55
M2	5.445	0.0583	0.88		47.94
M3	3.579	0.1002	0.87		16.90
Non-linear Elovich	A, mg × g^{-1} min^{-1}	B, mg × min^{-1}	R^2		χ^2
M0	1.252	0.0701	0.95		11.44
M1	3.671	0.0810	0.88		40.43
M2	4.944	0.0603	0.91		56.63
M3	3.313	0.0981	0.91		19.64

Summarizing the kinetic models applied in the present work, the adsorption of MB onto cellulose derivative composite membranes was better fitted by the non-linear PFO model, followed by the PSO model, and then non-linear PSO. The same order of model fittingness was observed for methyl orange adsorption onto bentonite (MO/Bt).[39]

3.3 *Linear and non-linear Langmuir and Freundlich isotherm models*

Adsorption occurs by the "donor-acceptor" complex formation mechanism where atoms of the surface functional

groups donate electrons to the adsorbate. The position of these functional groups on the adsorbent surface influences the type of adsorbate/adsorbent bond and, therefore, determines whether the process is physisorption or chemisorption.[40]

Accordingly to the Langmuir[41] and Freundlich[42] models, expressed in the linear and non-linear forms, Equations (13)-(16), it is assumed the Langmuir isotherm as monolayer adsorption, with adsorption occurring at a finite number of specific localized sites, without interactions between the adsorbed molecules, while the Freundlich isotherm can be applied to multilayer adsorption, with non-uniform distribution of adsorption heat and affinities over the heterogeneous surface.

$$\frac{C_e}{q_e} = \frac{C_e}{q_m} + \frac{1}{q_m K_L} \tag{13}$$

$$q_e = \frac{q_m \times K_L \times C_e}{1 + K_L \times C_e} \tag{14}$$

$$\ln(q_e) = \ln(K_F) + \frac{1}{n} \times \ln(C_e) \tag{15}$$

$$q_e = K_F \times C_e^{\frac{1}{n}} \tag{16}$$

The easy method to solve the isotherms is to transform the equations into a linear form so that the constants can be easily calculated by applying the linear regression analysis. The linear models (Figure 3 (a) and (b); Table 5) for both models, achieved by the software Origin 2024 (free trial license), showed well-defined straight lines with high linear regression coefficients ($R^2 = 0.97 – 0.99$) for all tested membranes and very low values of Chi-square were achieved.

The linear regressions of the Langmuir model, Figure 3 (a), gave high values of R^2 and small values of chi-square, and a high monolayer capacity towards MB (M0: 757.6 mg × g^{-1}; M1: 78.43 mg × g^{-1}; M2: 124.8 mg × g^{-1}; and M3 67.75 mg × g^{-1}). In Figure 3 (b), the experimental data fitted by the Freundlich linear form showed high values of R^2 and lower values of chi-square, which confirms the ability of the linear model to represent the data shown. Besides the values of n were higher than 1 ($0 < 1/n < 1$) indicating a favourable adsorption isotherm.

Considering these results, it is assumed the linear isotherm models as good models to describe the adsorption onto membranes. A possible explanation for the observed is the adsorption of dye molecules could be done through a parallel position, without interactions between each other, on the adsorbent surface and a monolayer forms on the adsorbent surface. It is more likely to occur under lower concentrations of adsorbate. But if dye molecules interact on a vertical position with the surface of the investigated adsorbent, a multi-molecular process is predominant. This effect is more common under higher concentrations of adsorbate. The same behavior was observed for example in the methylene blue adsorption onto chitosan-montmorillonite/polyaniline nanocomposite[29] and adsorption of methylene blue on agroindustrial wastes.[43]

By using the non-linear Langmuir model the solute adsorptivity (K_L) and the adsorption capacity of the monolayer (q_m) parameters were found of similar magnitude to the linear model (Figure 3 (c); Table 5). As well, the chi-square values indicated good fittingness and the graph confirmed the suitability of the non-linear Langmuir model. The same analysis was not applicable to the non-linear Freundlich model since the chi-square values were much higher than the values obtained with the linear model. As a final note, the nonlinear Langmuir model was better than Freundlich as was explained for As (V) adsorption on hematite.[44] The better performance of the Langmuir isotherm can be explained by the fact that chemisorption is the predominant process of adsorption of MB onto membranes.

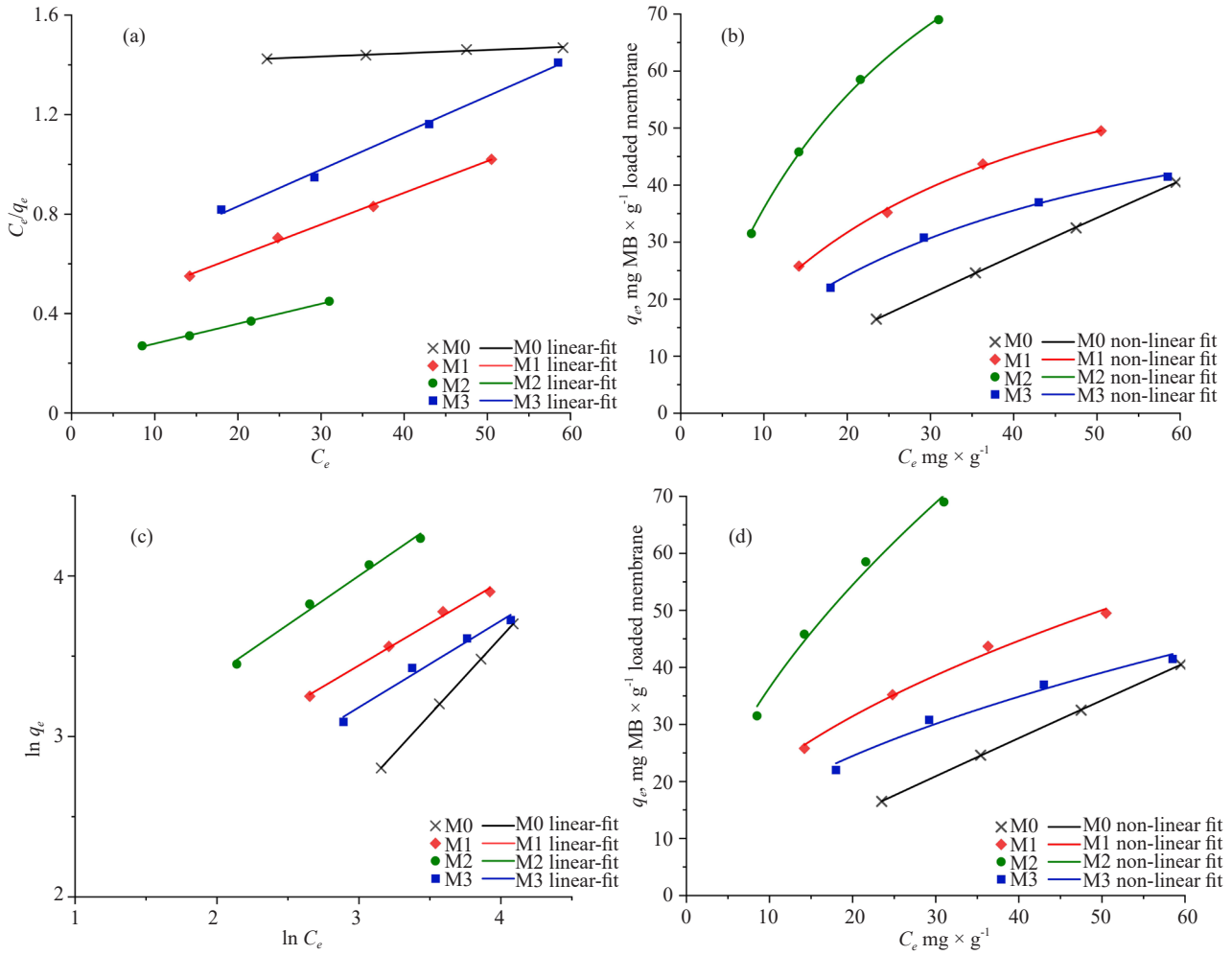

Figure 3. Experimental data and linear and non-linear isotherm models, respectively: (a, b) Langmuir and (c, d) Freundlich models for MB adsorption on composite membranes

Table 5. Parameters calculated from various isotherm models (initial MB concentration = 100 mg × L^{-1}, membranes = 25 mg, pH = 7.0, temperature = 25 °C)

Langmuir	Linear model				Non-linear model			
	K_L (L × mg^{-1})	q_m, mg × g^{-1}	R^2	χ^2	K_L (L × mg^{-1})	q_m, mg × g^{-1}	R^2	χ^2
M0	9.47E-4	757.6	0.97	3.511E-6	8.76E-4	816.3	0.99	9.493E-3
M1	3.40E-2	78.43	0.99	2.624E-5	3.37E-2	78.67	0.99	3.335E-1
M2	1.49E-2	124.8	0.99	2.635E-6	4.08E-2	124.0	0.99	2.551E-1
M3	2.76E-2	67.75	0.99	8.070E-5	2.79E-2	67.45	0.99	3.603E-1
Freundlich	K_F (L × mg^{-1})	n	R^2	χ^2	K_F (L × mg^{-1})	n	R^2	χ^2
M0	0.785	1.04	0.99	1.522E-6	0.787	1.04	0.99	5.622E-3
M1	6.52	1.91	0.99	1.340E-4	6.87	1.97	0.99	1.19
M2	15.1	1.64	0.99	3.475E-4	9.60	1.72	0.99	3.98
M3	4.77	1.85	0.98	4.341E-4	5.29	1.95	0.98	2.01

Other researchers reported similar observations for the adsorption of MB onto different adsorbents. Table 6 lists a comparison of the maximum adsorption capacities of the samples used in this study with various adsorbents previously studied.[28-29,45-47] It can be seen that the hematite-cellulose membranes show higher adsorption ability and better kinetic parameters than most adsorbents reported in literature.

Table 6. Comparison of the MB adsorption capacity of hematite-cellulose derivative membranes and some other available adsorbents

Adsorbent (ads)	Adsorption conditions				q_{exp}, mg × g^{-1}	q_m, mg × g^{-1}	k^2, g × mg^{-1}min^{-1}	Ref.
	C_0, mg × L^{-1} V, mL	m_{ads}, mg	pH	Temperature (K)				
Dopamine/cellulose acetate	50 20	10	6.5	298	88.2	165.84	0.0001117	45
Fe_3O_4/graphene	10 50	10	7	283	28.5	65.79	0.074	28
Carbon modified (SLS-C)	50 100	15	5	298	195.87	232.5	0.00157	46
Chitosan-montmorillonite/ polyaniline	20 100	50	13	298	130.67	111	0.0027	29
carbon/ montmorillonite	140 50	50	8	298	126.5	138.1	0.001	47
Fe_2O_3/cellulose acetate	100 25	25	7	25	69.1	127.4	0.000423	This study

3.4 *Evaluation of the thermodynamic parameters*

Thermodynamic parameters such as enthalpy change (ΔH^0), Gibbs free energy change (ΔG^0) and entropy change (ΔS^0) were determined by Equations 17 to 19[48-50] shown below. The T is the temperature (K), R is the universal gas constant (8.314 J × mol^{-1} K^{-1}), K_d (L × g^{-1}) is the standard thermodynamic equilibrium constant, q_e is the amount of adsorbed MB per unit mass of cellulosic membranes (mg × g^{-1}) and C_e is the equilibrium aqueous concentration of MB (mg × L^{-1}).

$$\Delta G = \Delta H - T\Delta S \tag{17}$$

$$\Delta G = -RT\ln(K_d), \text{ with } K_d = \frac{q_e}{C_e} \tag{18}$$

$$\ln K_d = \left(\frac{\Delta S}{R}\right) - \left(\frac{\Delta H}{RT}\right) \tag{19}$$

The values of ΔS^0, ΔH^0, and ΔG^0 were obtained from the slope and intercept of the plot between ln K_d versus $1/T$ (Equation 19). The calculated values are shown in Table 7. The negative value of ΔS^0 indicates a decrease of the random effect with increasing temperature due to the link between adsorbate and adsorbent. This means less entropy due to adsorption in progress. ΔH^0 is also negative which implies an exothermic reaction and evolution of heat as it is common in chemisorption and confirmed by the previous section. The value of enthalpy change was -90.44 kJ × mol^{-1}. Finally, the ΔG^0 was negative in the temperature range and became more negative with increasing temperature, implying that the amount adsorbed at equilibrium increased with increasing temperature. It negative sign indicates that the adsorption process was feasible and spontaneous,[13,26,51] which is the ideal process for industrial application as no energy is required to do the MB adsorption.

Table 7. Thermodynamic parameters for removal of MB onto M2

ΔS^0 (J × mol^{-1} K^{-1})	ΔH^0 (J × mol^{-1})	ΔG^0 (J × mol^{-1})		
		293	298	303
-297.7	-90,439.6	-177,665.7	179,154.2	-180,642.7

3.5 *Performance in desorption and reutilization*

Reutilization and regeneration of adsorbent and filter membranes are highly significant for practical applications, especially in industry, due to the necessity for reduction of the secondary pollution and overall costs.

Here, desorption experiments were performed on M2, the membrane with better performance for MB adsorption, to evaluate its reusability under "extreme" conditions (higher initial concentration of MB (100 mg × L^{-1}, appropriate water temperature (25 °C) and pH = 7. Between cycles, the adsorbent was washed with a basic solution.[18] The results shown in Figure 4 indicate a slight decrease in adsorption capacity after each cycle as some MB molecules could stay attached to the membrane surface as a consequence of bonds between the adsorbent and adsorbate as discussed above. Even though, chemisorption could be reversible, as proved by the colour and weight of the membrane after desorption. Consequently, the as-prepared magnetic membrane showed good recyclability and it is expected to be appropriate for up to 5 cycles of adsorption. This makes it a suitable system to be up-scaled and applied in more complex systems.

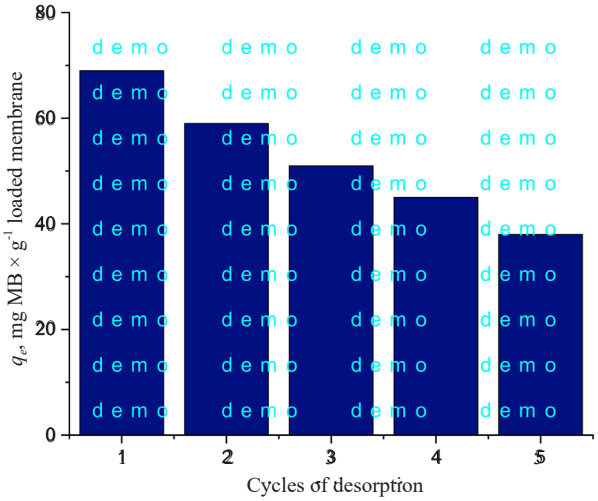

Figure 4. Adsorption capacity of MB on M2 (best performance) in five cycles (T = 25 °C; initial MB concentration = 100 mg × L^{-1}; pH = 7)

4. Box Behnken response surface methodology

In every industry, a correct modeling analysis is a fundamental tool for managing a process and in this study is important for the adsorption process as it can allow determining the performance of the system under any possible (and potentially infinite) operating conditions.

4.1 *Experimental results*

In this work, we have used a 3-factor, 3-level Box Behnken design (BBD), which needed 15 experimental runs. The experiments were performed based on the experimental runs made at different factor-level combinations. Table 2 shows the experimental matrix. The parameters corresponding to the central point (0, 0, 0) were repeated five times to guarantee normal dispersion and repeatability for the experimental data. To fit the response functions with the

experimental data, regression analysis was performed. The regression coefficients obtained for all the membranes are presented in Equations (20)-(27), in terms of coded factors and actual factors.

$$q = 26.9 + 10.4X_1 + 7.14X_2 - 4.55X_3 - 4.11X_1^2 - 3.26X_2^2 + 3.52X_1 \times X_2 \quad (20)$$

$$q = -5.49 + 6.21\text{pH} + 0.510C_{dye} - 0.910T - 0.457\text{pH}^2 - 0.00362C_{dye}^2 + 0.00392\text{pH} \times C_{dye} \quad (21)$$

$$q = 30.1 + 21.5X_1 + 7.24X_2 - 4.37X_3 - 4.68X_1^2 - 3.89X_2^2 - 2.76X_3^2 + 6.48X_1 \times X_2 - 3.46X_1 \times X_3 \quad (22)$$

$$q = -121 + 14.1\text{pH} + 0.415C_{dye} + 6.02T - 0.520\text{pH}^2 - 0.00433C_{dye}^2 - 0.110T^2 + 0.0719\text{pH} \times C_{dye} - 0.231\text{pH} \times T \quad (23)$$

$$q = 43.0 + 26.6X_1 + 7.26X_2 - 2.20X_3 - 10.1X_1^2 - 6.30X_2^2 - 4.70X_3^2 + 5.48X_1 \times X_2 \quad (24)$$

$$q = -183 + 18.1\text{pH} + 0.857C_{dye} + 8.96T - 1.128\text{pH}^2 - 0.00700C_{dye}^2 - 0.188T^2 + 0.0609\text{pH} \times C_{dye} \quad (25)$$

$$q = 31.0 + 19.8X_1 + 6.78X_2 - 4.34X_3 - 6.03X_1^2 - 5.31X_2^2 - 4.19X_3^2 + 5.89X_1 \times X_2 - 3.78X_1 \times X_3 \quad (26)$$

$$q = -171 + 16.4\text{pH} + 0.659C_{dye} + 9.03T - 0.670\text{pH}^2 - 0.00590C_{dye}^2 - 0.168T^2 + 0.0654\text{pH} \times C_{dye} - 0.252\text{pH} \times T \quad (27)$$

The obtained models (in terms of coded factors and actual factors) show that temperature had a negative effect on the amount of MB adsorbed, as seen from the thermodynamic tests, while an increase in MB initial concentration and pH increased the amount adsorbed as shown, previously. Besides the individual effects, it was also seen as a positive effect on the removal of MB in terms of the interaction effects between MB initial concentration and pH. This can be explained by the positive effect of both parameters on the adsorption efficiency. Conversely, the negative interaction effect between pH and temperature is explained by the negative effect of temperature. The double interaction effects of pH, concentration and temperature were negative on MB adsorbed, meaning that an increase in any of these parameters brought down the amount of MB adsorbed.

However, attending to the equations and their coefficients, it is presumed that the pH has a higher influence on MB adsorbed comparatively to other parameters. This effect is very common when we deal with charged molecules. However, to obtain a good removal efficiency of MB its initial concentration should be increased. It is notorious that in these models there are certain factors, specifically the interaction double factors, with very low values, indicating that they can be not influential. To discern this situation, the following statistical analysis of the factors is necessary to answer this question.

4.2 *Confidence level by analysis of variance*

Analysis of variance (ANOVA) is relevant to evaluate the significance of the factors in the response, at a confidence level of 95%. ANOVA data on M0 is reported in Table 8. The corresponding analysis values for M1, M2 and M3 are presented in the Supplementary Information (Tables S1-S3).

The data in Table 8 show that the obtained equations for the factors used in this study adequately represented the actual relationship between each response and the significant factors. The *F*-value in the models is significant and the values of the *Prob* > *F* are less than 0.05. From the *p*-values ($p < 0.05$) it is assumed that the quadratic model fitted the experimental data well as expected from the first part of the study (adsorption tests).

In this study, the *F*-values obtained were 69.81 for M0, 108.27 for M1, 123.34 for M2 and 170.77 for M3, indicating that the models were significant for all membranes. In addition, X_1, X_2, X_3, and their first and second-order interactions were also significant model terms with significant *F*-values. Thus, we confirm that the described parameters are all statistically significant in MB removal.

Table 8. ANOVA of the removal efficiency of MB onto M0

Source	Sum of Squares (SS)	Degree of freedom (DF)	Mean Square (MS)	*F*-value	*p*-value *Prob* > *F*	Remarks
Model	1,585.81	6	264.302	69.81	0.000	Significant
X_1	867.36	1	867.361	229.10	0.000	Significant
X_2	407.55	1	407.551	107.65	0.000	Significant
X_3	165.62	1	165.620	43.75	0.000	Significant
$X_1 \times X_2$	49.70	1	49.702	13.13	0.007	Significant
X_1^2	62.73	1	62.730	16.57	0.004	Significant
X_2^2	39.46	1	39.465	10.42	0.012	Significant
Residual	30.29	8	3.786	-	-	-
Lack of fit	30.29	6	5.048	non-significant	non-significant	-
Pure Error	0.000	2	0.000	-	-	-
Total	1,616.10	14	-	-	-	-

4.3 *Models diagnosis*

The actual vs predicted adsorption capacity data for MB is presented in Table 9. The values of the regression coefficient, R^2, and the adjusted R^2, R_{adj}^2, were 98% and 97%, respectively, on M0. On M1, M2 and M3, both values were also higher and a smaller discrepancy between them. These values are very relevant to the confidence of the analysis as the R^2 value exemplifies to what extent the models can absolutely estimate the experimental data, and the adjusted value signifies the variation of mean described by the models.[18,20-21,27] Therefore, the correlations between the theoretical and experimental responses, calculated by the obtained models, were very satisfactory. By the other side, the predicted R^2, R_{pred}^2, was 89% on M0, 95% on M1, 93% on M2 and 96% on M3. Thus 95% of the response can be well predicted by the models on composite membranes, indicating that all the terms which were considered in the models were significant enough to make acceptable predictions.

Table 9. Summary of the regression analysis of the responses of membranes

Quadratic model	R^2	Adjusted R^2	Predicted R^2
Y : M0	0.9813	0.9672	0.8903
Y : M1	0.9913	0.9839	0.9475
Y : M2	0.9920	0.9839	0.9291
Y : M3	0.9956	0.9898	0.9593

4.4 *Box Behnken response surface contour plots*

The graphical representation of the response surface for the adsorbed amount of MB in relation to the three factors studied (pH, initial concentration of MB, and temperature) was used to understand interactions between variables and determine the optimal level of each variable for maximum MB adsorption. The mathematical model for describing the evolution of responses through 2D and 3D plots is shown in Figure 5 (a)-(f). These plots can only express two independent variables at a time against the response.

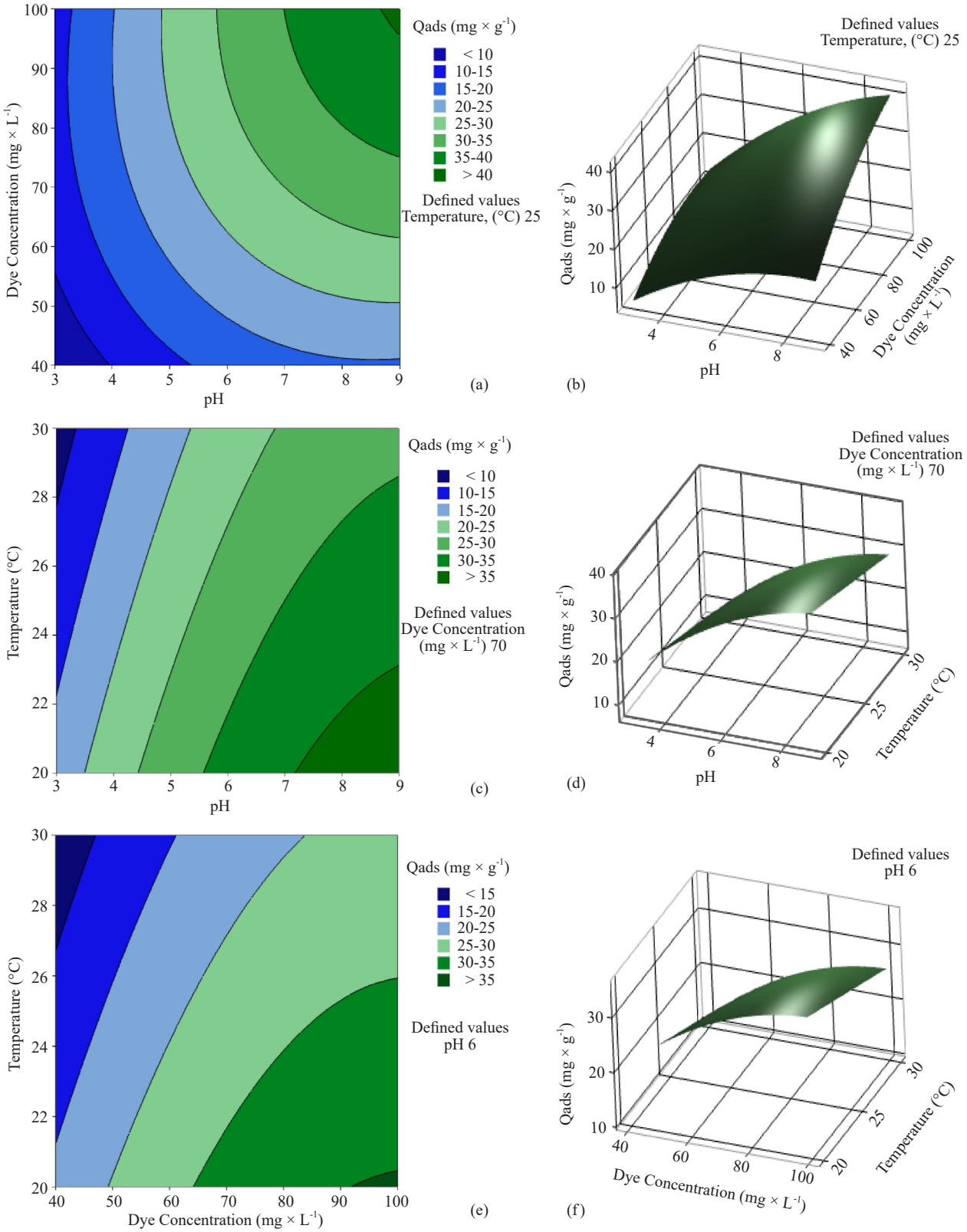

Figure 5. Representation of the two-dimensional and three-dimensional analysis plots (2D- and 3D-plots) of the adsorbed amount depending on two factors: (a)-(b) pH and concentration of MB, (c)-(d) pH and temperature, and (e)-(f) concentration of MB and temperature

The individual and combined effects of the three factors on MB adsorption capacity onto M0 were investigated and the response surface methodology was used. The effects of the experimental factors are represented in Figure 5 (a)-(f) through two- and three-dimensional plots. The response model is presented in Equation (20). The pH, initial MB concentration, and temperature significantly affected MB adsorption. The analysis shows that pH (X_1) has a major effect on MB adsorption capacity compared to other variables, as indicated by the high F-value for pH. However, the combined effects of the variables are not significant. The response surface method was used to analyse the three-dimensional response plots for the effect of all process variables on MB adsorption. Table 8, shows that pH and initial MB concentration were significant in increasing the effectiveness of the adsorbent in terms of adsorption capacity (Y). Figure 5 (a)-(f) illustrates the collective effect of all independent parameters on the adsorption capacity. The values on the figures' axes represent the real values.

Figure 5 (a)-(b) shows the interaction between pH (X_1) and initial MB concentration (X_2) on MB adsorption capacity at 300 min and 25 °C. The values for each variable were within the studied range of pH, initial MB concentration, and temperature. MB adsorption capacity increased sharply with an increase in pH and initial MB concentration. Increasing pH increased negative charges on the adsorbent surface with the enhancement of the interaction between MB cationic species and adsorbent active sites. Similarly, increasing MB concentration increased the available MB cationic species in the solution. Both, pH and MB concentration, synergistically affect MB adsorption capacity.

Figure 5 (c)-(d) demonstrates the combined effect of pH (X_1) and system temperature (X_3). As the system is exothermic, lower temperatures favoured the adsorption process. Increasing temperature decreased the activity of functional groups and decrease the complex formation. System temperature had a negative effect on MB adsorption, while pH had a positive effect. One effect was synergistic, while the other was antagonistic.

Figure 5 (e)-(f) represents the combined effect of initial MB concentration (X_2) and system temperature (X_3). Again, one effect was synergistic, while the other was antagonistic. When both parameters are at their maximum condition, MB adsorption capacity is minimum at any particular concentration. This was observed during the experimental trial.

Only the experimental data required for software optimization are presented here. However, it is evident from Table 8 and the 3D-response plot that pH (X_1) has a higher control over adsorption capacity compared to other parameters. Supplementary Information (Figures S1-S9) contain plots for M1, M2, and M3. A similar analysis can be made for them.

4.5 *Box Behnken response surface modelling and optimization*

The optimum conditions for maximum MB adsorption capacity onto the composite membranes were determined by the Box Behnken RSM technique.

The optimum operating conditions for the proposed membranes were found at the pH = 9, MB initial concentration = 100 mg × L^{-1} and T = 20 °C, with a corresponding desirability (d) value of 1. The experimental and predicted MB adsorption capacity at the optimum conditions are shown in Table 10. The error obtained between predicted models and the actual values was 2.8% for M0, 2.1% for M1, 2.0% for M2, and 1.9% for M3. On the basis of the results, we assume that these conditions are suitable for the development of a pilot-scale adsorption process.[18,21,23]

Table 10. Optimum conditions for the MB adsorption capacity on the composite adsorbent

Adsorbent	Batch conditions	MB adsorption capacity (q, mg × g^{-1})	
		Predicted (d = desirability)	Experimental
M0	pH = 9	45.3 (1.0)	46.1
M1	MB initial conc. = 100 mg × L^{-1}	61.8 (0.95)	60.5
M2	T = 20 °C	78.4 (1.0)	80.1
M3	-	56.0 (0.86)	57.1

5. Adsorbent cost estimation

Pilot-scale tests for dye removal using the prepared samples have not been conducted yet, so it is difficult to estimate the overall cost. At present, only the cost of raw materials was considered in the analysis. The cost of cellulose acetate used in the procedure was approximately US$ 0.018 per gram. Hematite nanoparticles and iron chloride powder were also used, with costs of US$ 0.13 per gram and US$ 0.13 per gram, respectively. Other raw materials were easily and cheaply obtained from industrial supplies. The cost of preparing the magnetic cellulosic composite adsorbents mainly depends on the cost of cellulose derivatives. Table 11 shows a comparison to other adsorbents, considering only the cost of raw materials. It is seen that our adsorbents have a compatible cost or are even smaller than most of the adsorbents cited in the literature. Furthermore, magnetic cellulosic composites have efficient adsorption properties and regeneration abilities, making it much more attractive.

Table 11. Costs of the materials used in the preparation of adsorbents mentioned in Table 6

Materials for adsorbent	Supplier	Link	Price (US$)/kg
Cellulose acetate, 99%, powder	Hebei Haojiang Technology Co. Ltd.	https://hbfengqiang.en.made-in-china.com/	US$ 10-50
Dopamine Hydrochloride, 99%, powder	Hebei Haojiang Technology Co. Ltd.	https://hbfengqiang.en.made-in-china.com/	US$ 10
Chitosan, powder (quality: industry)	Jinan Future Chemical Co., Ltd.	https://jnfuturechemical.en.made-in-china.com/	US$ 20-50
Montmorillonite, powder (quality: industry)	HaiHang Industry Co., Ltd.	https://haihangindustry.en.made-in-china.com/	US$ 60-100
Polyaniline, powder (quality: industry)	Shandong Huachuang New Material Technology Development Co., Ltd.	https://bac7aa36dfbdbeb9.en.made-in-china.com/	US$ 1-15
Graphene Oxide, 98%, powder	Hebei Rongxintong Industrial Co., Ltd.	https://rxtchem.en.made-in-china.com/360-Virtual-Tour.html	US$ 0.23-0.32
Activated Carbon, Granular, Powder, Pellet, (quality: industry)	Zhengzhou Zhulin Activated Carbon Development Co., Ltd.	https://zhulincarbon.en.made-in-china.com/	US$ 0.12-0.20

6. Conclusions

The present study demonstrates that a cellulosic matrix modified by hematite nanoparticles, lab-made materials with low cost and safe for the environment, is a suitable alternative to most of the commonly used adsorbents made of carbon, zeolites and clays.

The kinetic studies of the adsorption of MB onto hematite cellulose membranes were better fitted by the non-linear PFO model, followed by the PSO model, and then non-linear PSO.

For the equilibrium data analysis, both the Langmuir and Freundlich models were able to explain the adsorption of MB onto the composite membranes. Firstly it is presumed that was reached the formation of a monolayer, followed by a multi-molecular adsorption process. The non-linear Langmuir model was also suitable for fitting experimental data confirming the chemisorption process. This process was exothermic and spontaneous as revealed by the obtained thermodynamic parameters.

The Box Behnken Response Surface Design used in analysing the effects of different formulation variables on the adsorption capacity suggested that the BBD was a suitable method for understanding the effect of each factor (dependent variables, Xi) and optimizing/increasing the independent factor (adsorption capacity, Y). The desirability function (d) for the optimized responses was close to 1 and showed a close agreement with the experimental data.

In conclusion, hematite cellulose membranes can be assumed as advantageous adsorbents for removing MB from aqueous media due to their low-cost production, partial biodegradability, recyclability and high efficiency for cationic molecules. In the future, these adsorbents can be used for adsorbing binary and ternary mixtures of dye molecules and their removal scaled up to pilot-scale processes.

Declaration of author contributions

This work is an original study, and therefore M. A. Silva has written the full manuscript draft based on her experimental design, investigation, data collection and analysis, etc.

Acknowledgments

M. Silva acknowledges funding for this study through an Individual postdoctoral grant from Fundação para a Ciência e a Tecnologia (PROJECT UID/CTM/00264/2013).

Confilict of interest

The author declares no competing financial interest.

References

[1] WHO Library Cataloguing-in-Publication Data Guidelines for drinking-water quality, 4th ed. 2011. https://www.iasaude.pt/attachments/article/660/WHO_Guidelines%20for%20drinking-water%20quality.pdf (accessed November 2023).
[2] EPA Home Page. https://www.epa.gov/laws-regulations/summary-clean-water-act (accessed November 2023).
[3] Australian Drinking Water Guidelines 6. 2011. https://www.nhmrc.gov.au/sites/default/files/documents/reports/aust-drinking-water-guidelines.pdf (accessed November 2023).
[4] Directive 2000/60/EC of the European Parliament and of the Council of 23 October 2000 establishing a framework for Community action in the field of water policy. https://eur-lex.europa.eu/eli/dir/2000/60/oj (accessed November 2023).
[5] European Comission: Energy, Climate Change, Environment Home Page. https://environment.ec.europa.eu/strategy/zero-pollution-action-plan_en (accessed November 2023).
[6] Guidance for Pollution Prevention Works and Maintenance in or Near Water: GPP 5 Version 1.2. 2018. https://www.netregs.org.uk/media/1418/gpp-5-works-and-maintenance-in-or-near-water.pdf (accessed November 2023).
[7] Khodaie, M.; Ghasemi, N.; Moradi, B.; Rahimi, M. *J. Chem.* **2013,** *2013*, 1-6.
[8] Dardouri, S.; Sghaier, J. *Kor. J Chem. Eng*. **2017,** *34*, 1037-1043.
[9] Ahmad, R.; Kumar, R. *J. Environ. Manage*. **2010,** *91*, 1032-1038.
[10] Moorthy, A. K.; Rathi, B. G.; Shukla, S. P.; Kumar, K.; Bharti, V. S. *Environ. Toxicol. Pharmacol*. **2021,** *82*, 103552.
[11] Valli Nachiyar, C.; Rakshi, A. D.; Sandhya, S.; Britlin Deva Jebasta, N.; Nellore, J. *Case Stud. Chem. Environ. Eng*. **2023,** *7*, 100339.
[12] Silva, M. A.; Hilliou, L.; de Amorim, M. T. P. *Polym. Bull*. **2020,** *77*, 623-653.
[13] Bingül, Z. *J. Mol. Struct*. **2022,** *1250*, 131729.
[14] Zhu, Y.; Yi, B.; Yuan, Q.; Wu, Y.; Wang, M.; Yan, S. *RSC Adv.* **2018,** *8*, 19917-19929.
[15] Oladoye, P. O.; Ajiboye, T. O.; Omotola, E. O.; Oyewola, O. J. *Results in Engineering* **2022,** *16*, 100678.
[16] Silva, M. A.; Felgueiras, H. P.; Amorim, M. T. P. *Cellulose* **2020,** *27*, 1497-1516.
[17] Silva, M. A.; Vieira Rocha, C.; Gallo, J.; Felgueiras, H. P.; Amorim, M. T. P. *Carbohydr. Polym*. **2020,** *241*, 116362.
[18] Silva, M. A.; Belmonte-Reche, E.; Amorim, M. T. P. *Fibers* **2021,** *9*, 61.
[19] Singh, B.; Kumar, R.; Ahuja, N. *Crit. Rev. Ther. Drug Carrier Syst*. **2005,** *22*, 27-106.
[20] Singh, B.; Bhatowa, R.; Tripathi, C. B.; Kapil, R. *Int. J. Pharm. Investig*. **2011,** *1*, 75-87.
[21] Marasini, N.; Yan, Y. D.; Poudel, B. K.; Choi, H. G.; Yong, C. S.; Kim, J. O. *J. Pharm. Sci*. **2012,** *101*, 4584-4596.
[22] Ferreira, S. L. C.; Bruns, R. E.; Ferreira, H. S.; Matos, G. D.; David, J. M.; Brandão, G. C.; da Silva, E. G. P.; Portugal, L. A.; dos Reis, P. S.; Souza, A. S.; et al. *Anal. Chim. Acta* **2007,** *597*, 179-186.
[23] Candioti, L. V.; De Zan, M. M.; Cámara, M. S.; Goicoechea, H. C. *Talanta* **2014,** *124*, 123-138.
[24] Rápó, E.; Tonk, S. *Molecules* **2021,** *26*, 5419.

[25] Paz, D. S.; Baiotto, A.; Schwaab, M.; Mazutti, M. A.; Bassaco, M. M., Bertuol, D. A.; Foletto, E. L.; Meili, L. *Water Sci. Technol*. **2013,** *68*, 441-447.
[26] Miyah, Y.; Lahrichi, A.; Idrissi, M.; Khalil, A.; Zerrouq, F. *Surf. Interfaces* **2018,** *11*, 74-81.
[27] Mbachu, C. A.; Babayemi, A. K.; Egbosiuba, T. C.; Ike, J. I.; Ani, I. J.; Mustapha, S. *Results Eng*. **2023,** *19*, 101198.
[28] Wang, P.; Cao, M.; Wang, C.; Ao, Y.; Hou, J.; Qian, J. *Appl. Surf. Sci*. **2014,** *290*, 116-124.
[29] Minisy, I. M.; Salahuddin, N. A.; Ayad, M. M. *Appl. Clay Sci.* **2021,** *203*, 105993.
[30] Lagergren, S. *Handlingar* **1898,** *24*, 1-39.
[31] Blanchard, G.; Maunaye, M.; Martin, G. *Water Res.* **1984,** *18*, 1501-1507.
[32] Ho, Y. S.; McKay, G. *Process Biochem.* **1999,** *34*, 451-465.
[33] Azizian, S. J. *Colloid Interface Sci.* **2004,** *276*, 47-52.
[34] López-Luna, J.; Ramírez-Montes, L. E.; Martinez-Vargas, S.; Martínez, A. I.; Mijangos-Ricardez, F.; González-Chávez, M. C. A.; Carrillo-González, R.; Solís-Domínguez, F. A.; Cuevas-Díaz, M. C; Vázquez-Hipólito, V. *SN Appl. Sci.* **2019,** *1*, 950.
[35] Guo, L.; Li, G.; Liu, J.; Meng, Y.; Xing, G. *J. Dispers. Sci. Technol*. **2012,** *33*, 403-409.
[36] Ho, Y. S. J. *Hazard. Mat.* **2006,** *136*, 681-689.
[37] Elovich, S. Y.; Larinov, O. G. *Izvestiya Akademii Nauk SSSR, Otdelenie Khimicheskikh Nauk* **1962,** *2*, 209-216.
[38] Chien, S. H.; Clayton, W. R. *Soil Sci. Soc. Am. J*. **1980,** *44*, 265-268.
[39] Moussout, H.; Ahlafi, H.; Aazza, M.; Maghat, H. *Karbala Int. J. Mod. Sci*. **2018,** *4*, 244-254.
[40] McKay, G. *Use of Adsorbents for the Removal of Pollutants from Wastewaters, 1st edn*. Tokyo, CRC: Boca Raton, 1996.
[41] Langmuir, J. J. *Am. Chem. Soc*. **1918,** *40*, 1361-1403.
[42] Freundlich, H. *Journal of Physics Zur Chemistry* **1906,** *57*, 384-470.
[43] Meili, L.; Lins, P. V. S.; Costa, M. T.; Almeida, R. L.; Abud, A. K. S.; Soletti, J. I.; Dotto, G. L.; Tanabe, E. H.; Sellaoui, L.; Carvalho, S. H. V.; et al. *Prog. Biophys. Mol. Biol*. **2018,** *141*, 60-71.
[44] Tang, W.; Li, Q.; Gao, S.; Shang, J. K. *J. Hazard. Mat.* **2011,** *192*, 131-138.
[45] Cheng, J. Q.; Zhan, C. H.; Wu, J. H.; Cui, Z. X.; Si, J.; Wang, Q. T.; Peng, X. F.; Turng, L. S. *ACS Omega* **2020,** *5*, 5389-5400.
[46] Kuang, Y.; Zhang, X.; Zhou, S. *Water* **2020,** *12*, 587.
[47] Tong, D. S.; Wu, C. W.; Adebajo, M. O.; Jin, G. C.; Yu, W. H.; Jin, G. C.; Yu, W. H.; Ji, S. F.; Zhou, C. H. *Appl. Clay Sci.* **2018,** *161*, 256-264.
[48] Moussavi, G.; Khosravi, R. *Chem. Eng. Res. Des.* **2011,** *89*, 2182-2189.
[49] Tsai, W. T.; Chang, Y. M.; Lai, C. W.; Lo, C. C. *J. Colloid Interface Sci*. **2005,** *289*, 333-338.
[50] Sprynskyy, M.; Buszewski, B.; Terzyk, A. P.; Namiesnik, J. J. *Colloid Interface Sci.* **2006,** *304*, 21-28.
[51] Sivarajasekar, N.; Baskar, R. *Arabian J. Chem.* **2019,** *12*, 1322-1337.

Supplementary information (SI)
Appendix A

Table S1. ANOVA of the removal efficiency of MB onto M1

Source	Sum of Squares (SS)	Degree of freedom (DF)	Mean Square (MS)	*F*-value	*p*-value *Prob* > *F*	Remarks
Model	4,641.08	8	580.14	108.27	0.000	Significant
X_1	3,709.19	1	3,709.19	692.25	0.000	Significant
X_2	419.05	1	419.05	78.21	0.000	Significant
X_3	152.78	1	152.78	28.51	0.002	Significant
$X_1 \times X_2$	167.70	1	167.70	31.30	0.001	Significant
$X_1 \times X_3$	47.89	1	47.89	18.94	0.024	Significant
X_1^2	80.96	1	80.96	15.11	0.008	Significant
X_2^2	55.94	1	55.94	10.44	0.018	Significant
X_3^2	28.08	1	28.08	5.24	0.062	Significant
Residual	32.15	6	5.36	-	-	-
Lack offit	32.15	4	8.04	non-significant	non-significant	-
Pure Error	0.000	2	0.000	-	-	-
Total	4,673.23	14	-	-	-	-

Table S2. ANOVA of the removal efficiency of MB onto M2

Source	Sum of Squares (SS)	Degree of freedom (DF)	Mean Square (MS)	*F*-value	*p*-value *Prob* > *F*	Remarks
Model	6,780.58	7	968.85	123.34	0.000	Significant
X_1	5,663.14	1	5,663.14	721.08	0.000	Significant
X_2	421.52	1	421.52	53.67	0.000	Significant
X_3	38.81	1	38.81	4.94	0.062	Significant
$X_1 \times X_2$	120.23	1	120.23	15.31	0.006	Significant
X_1^2	377.12	1	377.12	48.02	0.000	Significant
X_2^2	146.61	1	146.61	18.67	0.003	Significant
X_3^2	81.52	1	81.52	10.38	0.015	Significant
Residual	54.98	7	7.85	-	-	-
Lack offit	54.98	5	11.00	non-significant	non-significant	-
Pure Error	0.000	2	0.00	-	-	-
Total	6,835.56	14	-	-	-	-

Table S3. ANOVA of the removal efficiency of MB onto M3

Source	Sum of Squares (SS)	Degree of freedom (DF)	Mean Square (MS)	*F*-value	*p*-value *Prob* > *F*	Remarks
Model	4,108.58	8	513.57	170.77	0.000	Significant
X_1	3,130.38	1	3,130.38	1,040.89	0.000	Significant
X_2	367.88	1	367.88	122.33	0.000	Significant
X_3	150.51	1	150.51	50.05	0.000	Significant
$X_1 \times X_2$	138.65	1	138.65	46.10	0.000	Significant
$X_1 \times X_3$	57.00	1	57.00	18.95	0.005	Significant
X_1^2	134.31	1	134.31	44.66	0.001	Significant
X_2^2	103.96	1	103.96	34.57	0.001	Significant
X_3^2	64.94	1	64.94	21.59	0.004	Significant
Residual	18.04	6	3.01	-	-	-
Lack offit	18.04	4	4.51	non-significant	non-significant	-
Pure Error	0.000	2	0.00	-	-	-
Total	4,126.63	14	-	-	-	-

Appendix B

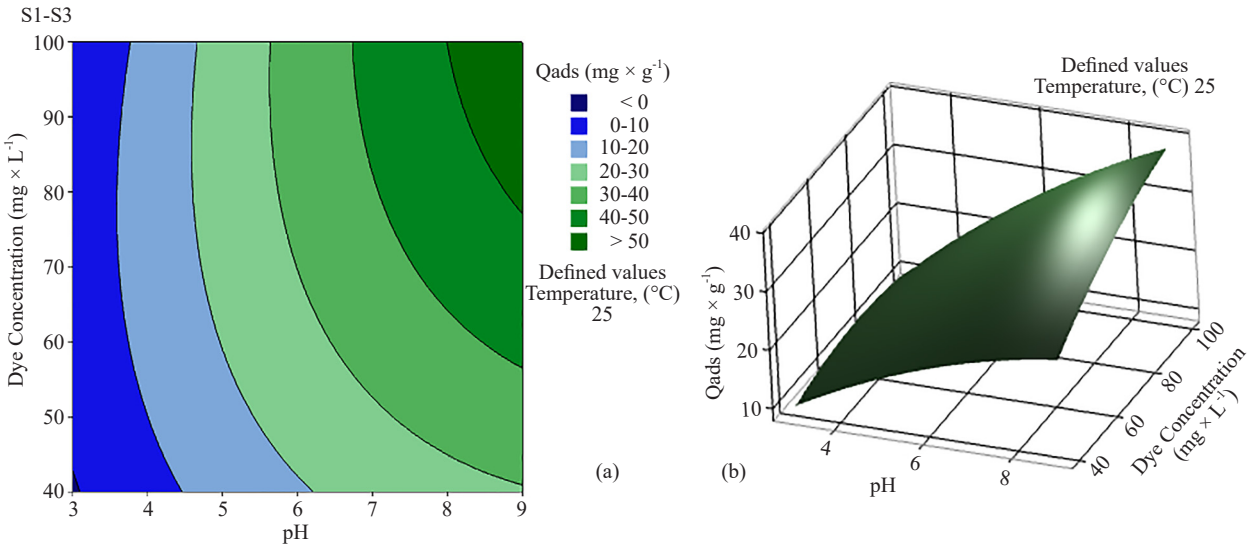

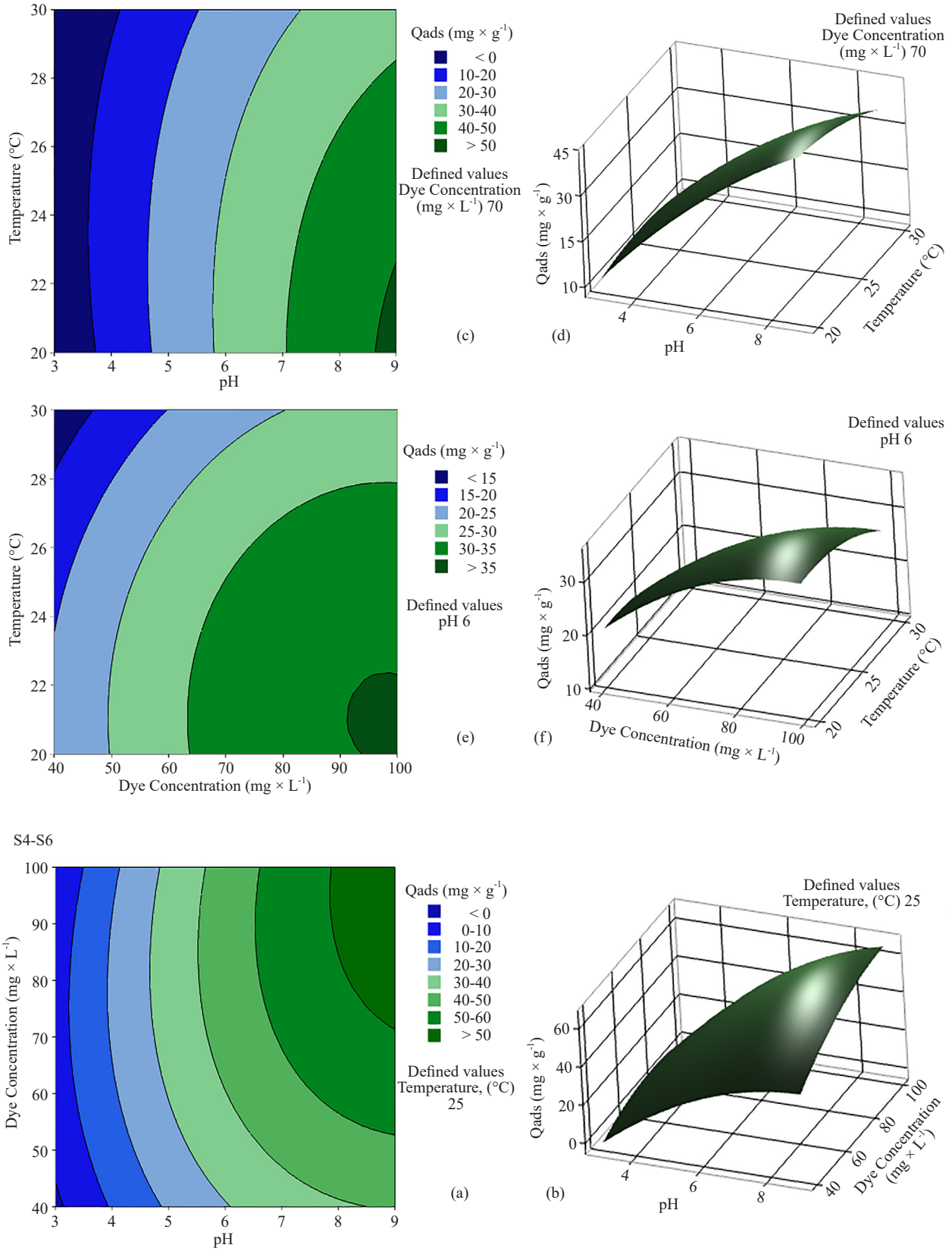
Temperature (°C)
pH
Qads (mg × g-1)
< 0
10-20
20-30
30-40
40-50
> 50
Defined values
Dye Concentration
(mg × L-1) 70
(c)
Qads (mg × g-1)
Defined values
Dye Concentration
(mg × L-1) 70
pH
Temperature (°C)
(d)
Temperature (°C)
Dye Concentration (mg × L-1)
Qads (mg × g-1)
< 15
15-20
20-25
25-30
30-35
> 35
Defined values
pH 6
(e)
Qads (mg × g-1)
Defined values
pH 6
Dye Concentration (mg × L-1)
Temperature (°C)
(f)
S4-S6
Dye Concentration (mg × L-1)
pH
Qads (mg × g-1)
< 0
0-10
10-20
20-30
30-40
40-50
50-60
> 50
Defined values
Temperature, (°C)
25
(a)
Qads (mg × g-1)
Defined values
Temperature, (°C) 25
pH
Dye Concentration
(mg × L-1)
(b)

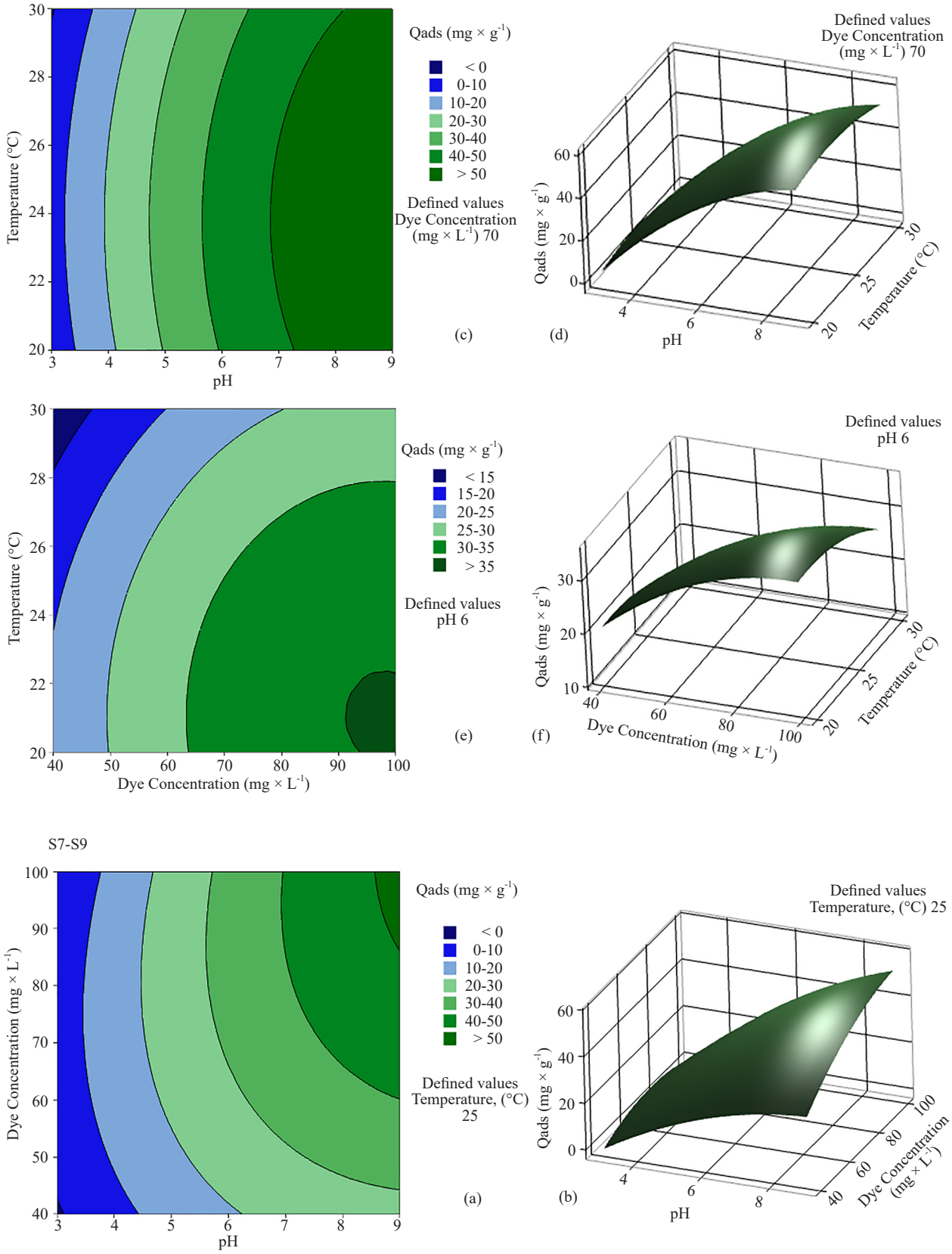
Temperature (°C)
pH
Qads (mg × g-1)
< 0
0-10
10-20
20-30
30-40
40-50
> 50
Defined values
Dye Concentration
(mg × L-1) 70
(c)
Defined values
Dye Concentration
(mg × L-1) 70
Qads (mg × g-1)
pH
Temperature (°C)
(d)
Temperature (°C)
Dye Concentration (mg × L-1)
Qads (mg × g-1)
< 15
15-20
20-25
25-30
30-35
> 35
Defined values
pH 6
(e)
Defined values
pH 6
Qads (mg × g-1)
Dye Concentration (mg × L-1)
Temperature (°C)
(f)
S7-S9
Dye Concentration (mg × L-1)
pH
Qads (mg × g-1)
< 0
0-10
10-20
20-30
30-40
40-50
> 50
Defined values
Temperature, (°C)
25
(a)
Defined values
Temperature, (°C) 25
Qads (mg × g-1)
pH
Dye Concentration
(mg × L-1)
(b)

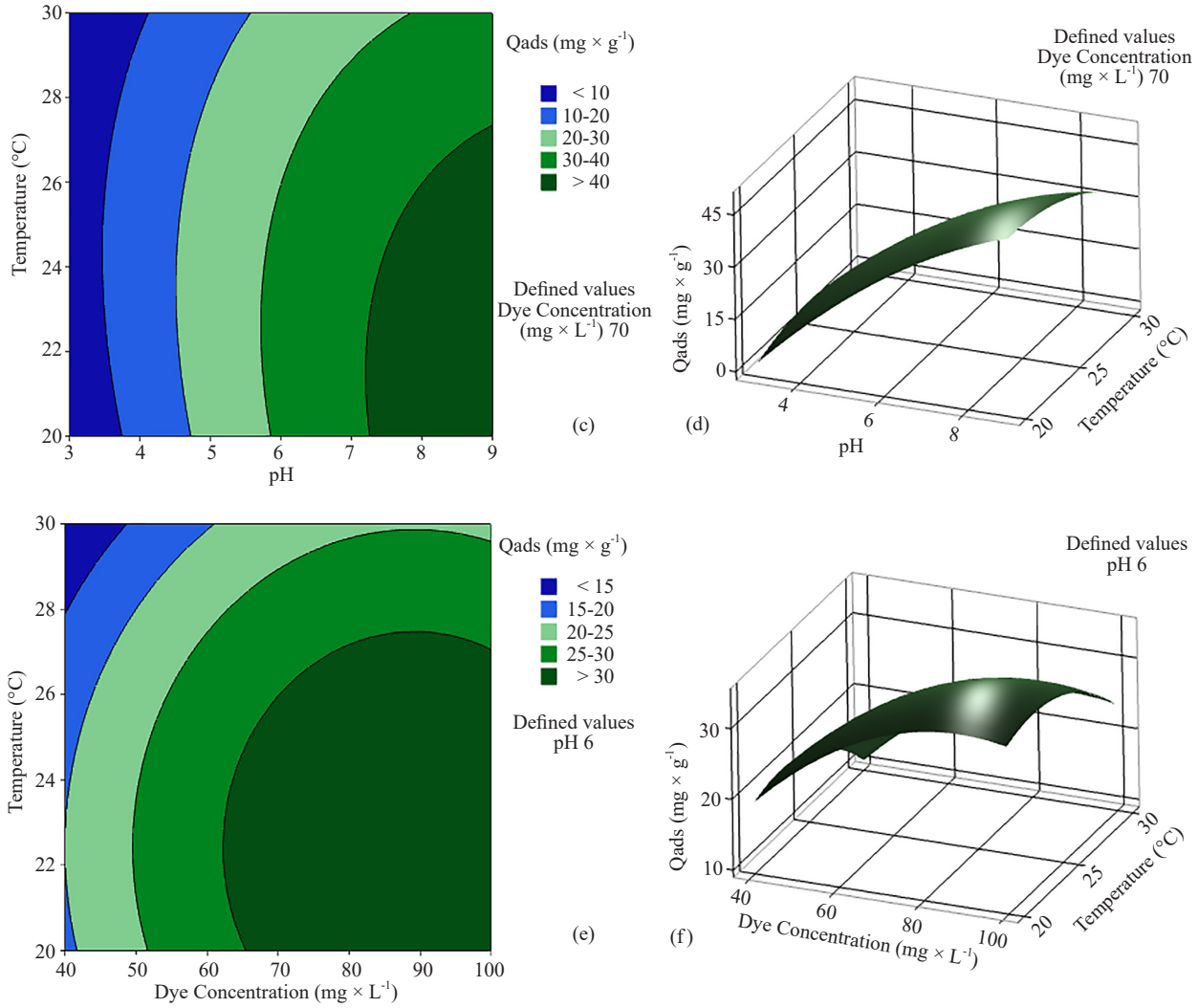

Figure S1-S9. Representation of the two-dimensional and three-dimensional analysis plots (2D- and 3D-plots) of the adsorbed amount depending on two factors: (a)-(b) pH and concentration of MB, (c)-(d) pH and temperature, and (e)-(f) concentration of MB and temperature for M1, M2 and M3, respectively